

Electronic Supplementary Information

Luminescent MOF as a fluorescent sensor for the sequential detection of Al³⁺ and phenylpyruvic acid

Qian Wang, Xiao-Meng Du, Bo Zhao, Meili Pang, Yue Li* and Wen-Juan Ruan*

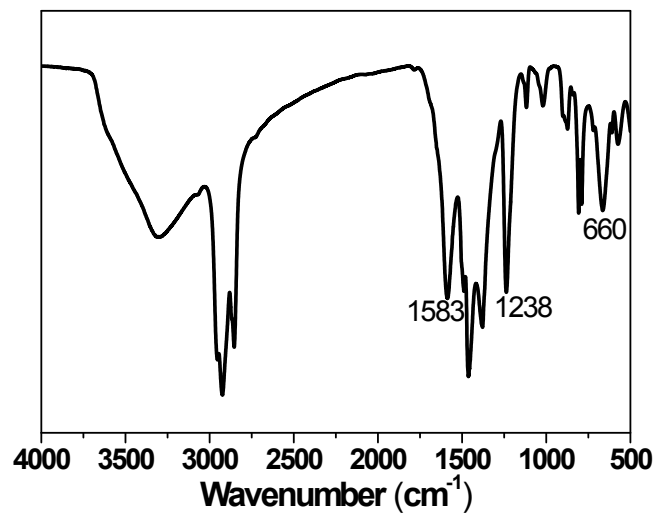


Fig. S1 FT-IR spectrum of as-prepared UiO-66-(OH)₂ sample. The intensive peak at 1238 cm⁻¹ could be assigned to the C-O stretching vibration of the hydroxyl groups on dhtp²⁻ ligand. The carboxyl groups gave absorption peak at 1586 cm⁻¹, instead of the range of 1650–1730 cm⁻¹, showing that it is completely deprotonated upon the formation of MOF structure.

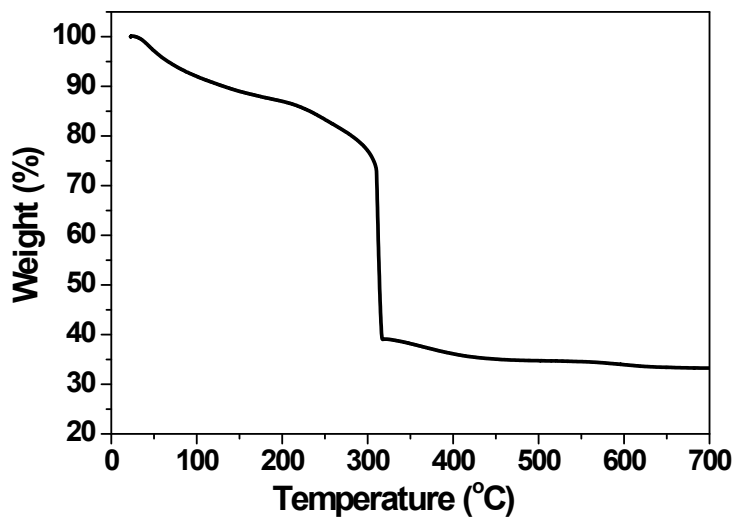


Fig. S2 Thermogravimetry curve of UiO-66-(OH)₂. The overall weight loss from room temperature to 700 °C is 66.8%, which is consistent with the loss of all H₂O molecules and organic components with ZrO₂ as residue (calcd 67.2%) based on the formula of [Zr₆O₄(OH)₄(dhtp)₆](DMF)₃(H₂O)₁₀.

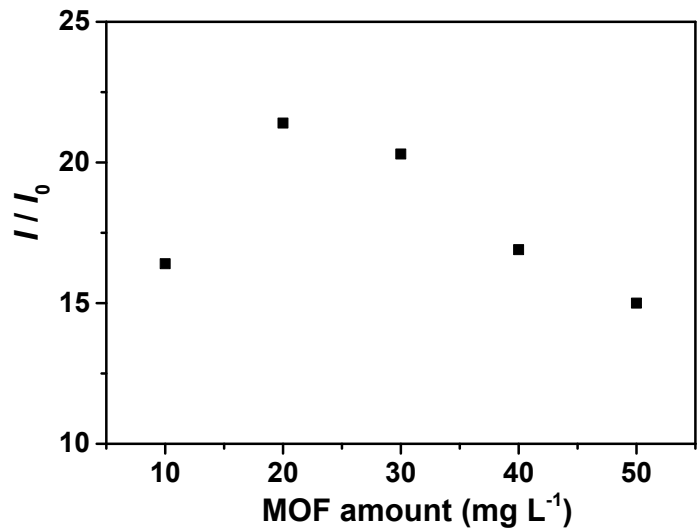


Fig. S3 Relative fluorescence enhancement induced by 50 μM Al^{3+} at different addition amounts of UiO-66-(OH)_2 .

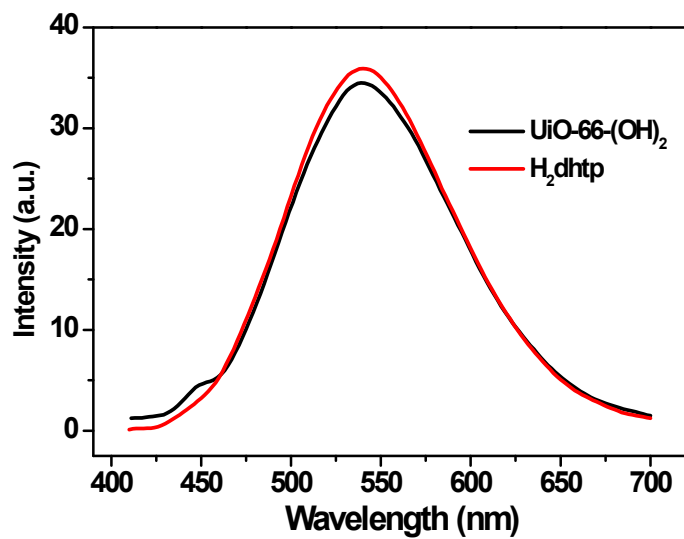


Fig. S4 Comparison between the fluorescence spectra of UiO-66-(OH)_2 (20 mg L^{-1}) and free H_2dhtp ligand (16 μM , dissolving H_2dhtp by 2 equiv. of NaOH) in aqueous media, $\lambda_{\text{ex}} = 385 \text{ nm}$.

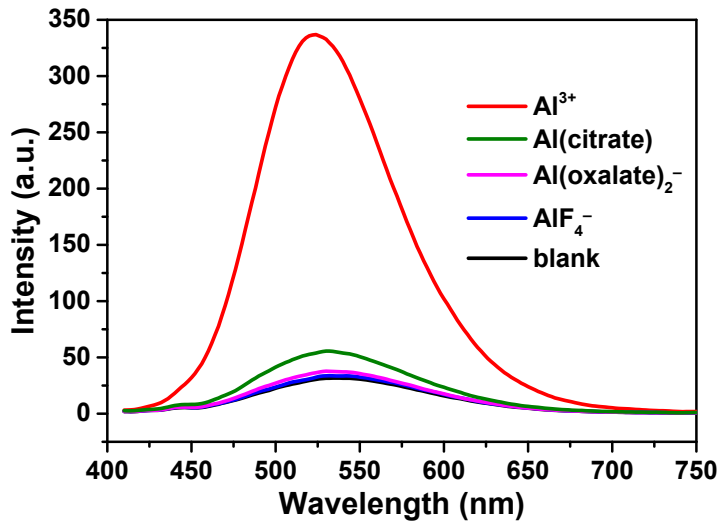


Fig. S5 Comparison among the fluorescent responses of UiO-66-(OH)_2 to Al^{3+} , AlF_4^- , $\text{Al}(\text{citrate})$ and $\text{Al}(\text{oxalate})^{2-}$.

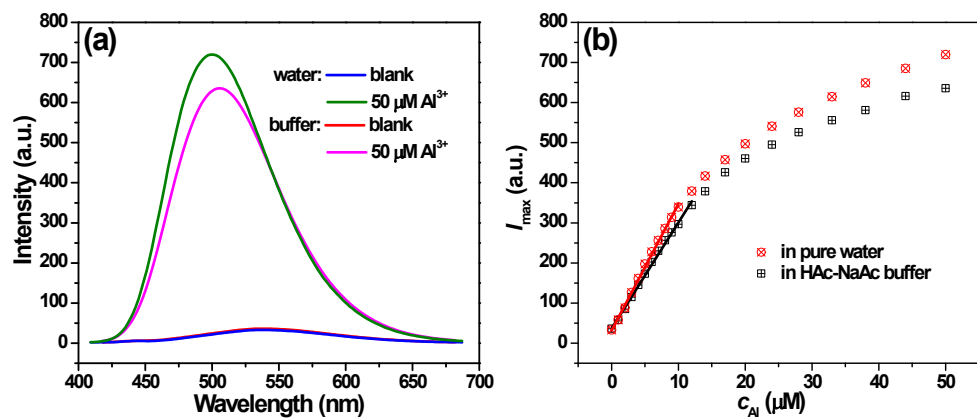


Fig. S6 Comparison between the changes of (a) fluorescent spectrum and (b) maximum emission intensity of UiO-66-(OH)_2 in pure water and HAc-NaAc buffer (10 mM, pH = 5.0) upon Al^{3+} addition.

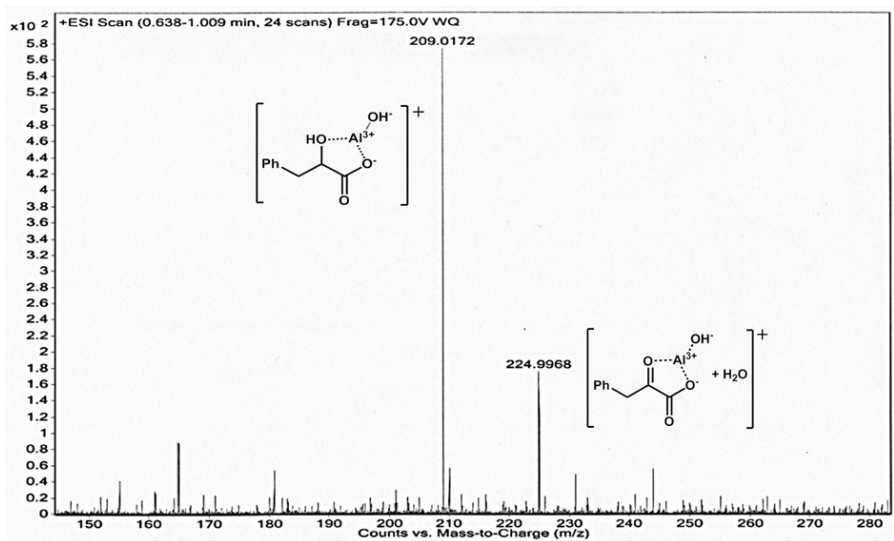


Fig. S7 ESI-MS spectrum of the solution after the sensing of PPA by $\text{UiO-66-(OH)}_2\text{-Al}^{3+}$, MOF sensor was separated by filtration.

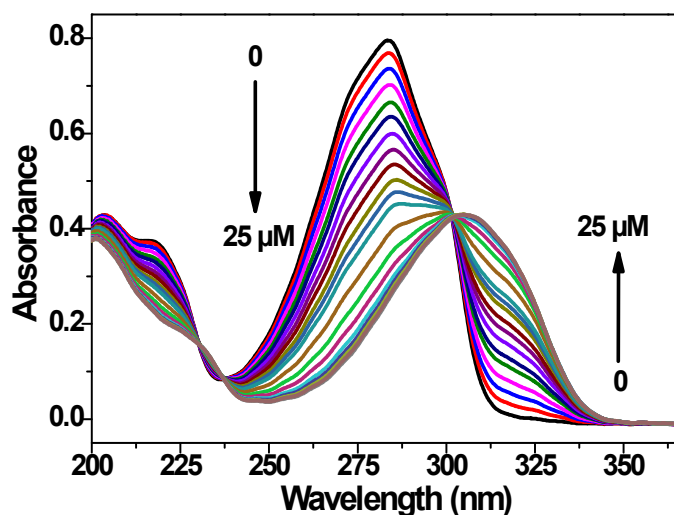


Fig. S8 UV-Vis spectra of PPA (50 μM) in the presence of Al^{3+} .

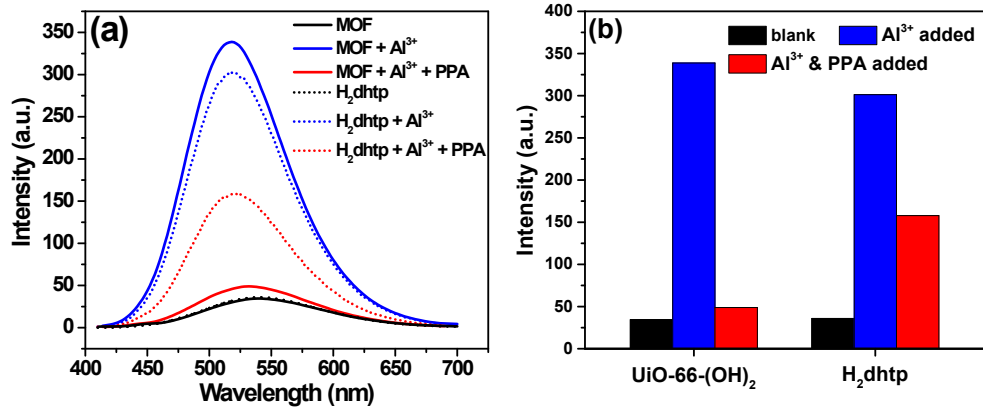


Fig. S9 (a) Fluorescent spectra of the suspension of UiO-66-(OH)₂ (20 mg L⁻¹) and the solution of H₂dhtp (16 μM) after the sequential addition of Al³⁺ (12 μM) and PPA (50 μM). (b) Comparison between the fluorescent responses of UiO-66-(OH)₂ and H₂dhtp.

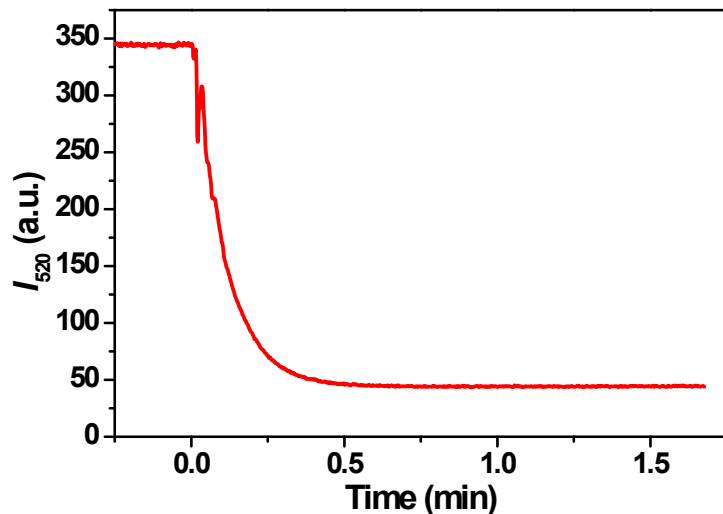


Fig. S10 Emission intensity change of UiO-66-(OH)₂-Al³⁺ after the addition of PPA (50 μM).

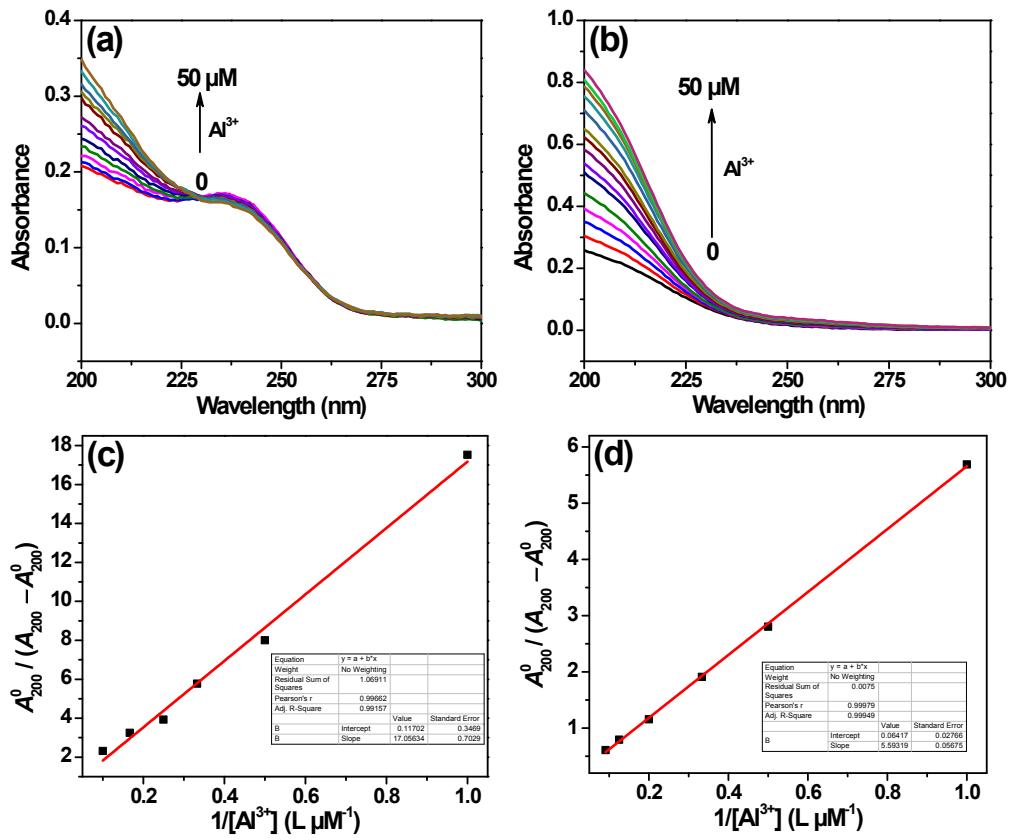


Fig. S11 Absorption spectra of (a) 100 μM pyruvic acid and (b) 100 μM α -ketoglutaric acid in the presence of different concentrations of Al³⁺. Linear fitting of the absorbance change of (c) pyruvic acid at 200 nm and (d) α -ketoglutaric acid at 200 nm with Al³⁺ addition based on Benesi-Hildebrand equation.

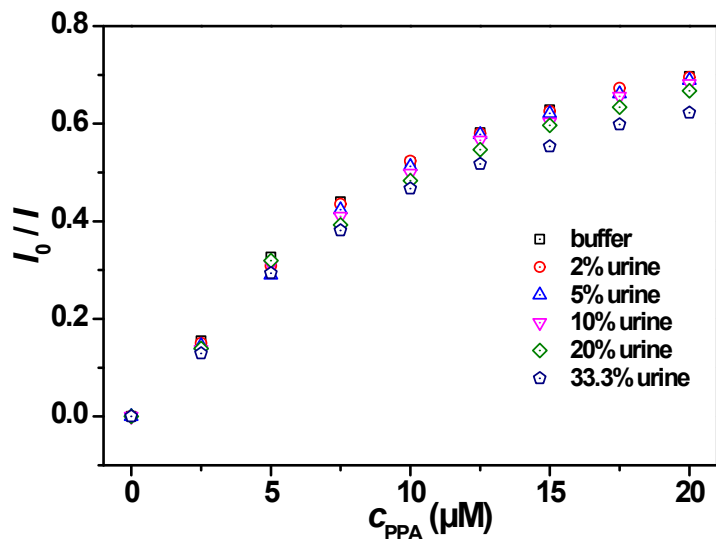


Fig. S12 Fluorescent response of $\text{UiO-66-(OH)}_2\text{-Al}^{3+}$ to PPA in dilutions of artificial urine.

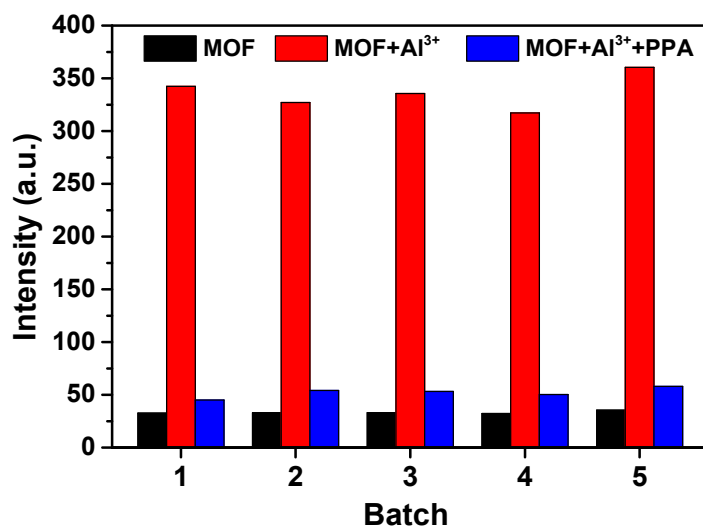


Fig. S13 Fluorescent responses of UiO-66-(OH)_2 samples from five different batches to Al^{3+} and PPA.

Table S1 Detection limits of recently reported Al³⁺ detection based MOF system.

Material	Mode	Detection limit	Ref.
TMU-60	colorimetric	3.7 μM	1
[Co ₂ (dmimpym)(nda) ₂] _n	fluorometric	0.7 μM	2
UiO-66-NH ₂ -SA	fluorometric	6.89 μM	3
[Tb(ppda)(ox) _{0.5} (H ₂ O) ₂] _n	fluorometric	5.66 μM	4
Mg-TPP-DHBDC	fluorometric	28 nM	5
[Eu(BTB)(phen)]	fluorometric	50 nM	6
UiO-66-(OH) ₂	fluorometric	47 nM	This work

Table S2 The quenching efficiencies of tested interfering substances on the emission of UiO-66-(OH)₂-Al³⁺.

Interfering substance	Concentration	1 - I/I ₀ (%)
cysteine	1 mM	-1.0
ascorbic acid	1 mM	9.2
phenylalanine	1 mM	0.1
sarcosine	1 mM	2.2
creatinine	1 mM	-0.5
hippuric acid	1 mM	3.7
urea	1 mM	0.2
uric acid	1 mM	7.1
pyruvic acid	50 μM	7.0
α-ketoglutaric acid	50 μM	12.3

References

1. F. Rouhani, F. Rafizadeh-Masuleh and A. Morsali, *J. Mater. Chem. A*, 2019, **7**, 18634–18641.
2. W. M. Chen, X. L. Meng, G.L. Zhuang, Z. Wang, M. Kurmoo, Q. Q. Zhao, X. P. Wang, B. Shan, C. H. Tung and D. Sun, *J. Mater. Chem. A*, 2017, **5**, 13079–13085.
3. S. Y. Zhu and B. Yan, *Dalton Trans.*, 2018, **47**, 1674–1681.
4. Z. Zhan, Y. Jia, D. Li, X. Zhang and M. Hu, *Dalton Trans.*, 2019, **48**, 15255–15262.
5. Y. P. Li, X. H. Zhu, S. N. Li, Y. C. Jiang, M. C. Hu and Q. G. Zhai, *ACS Appl. Mater. Interfaces*, 2019, **11**, 11338–11348.
6. H. Xu, B. Zhai, C. S. Cao and B. Zhao, *Inorg. Chem.*, 2016, **55**, 9671–9676.